



Structure and high dielectric permittivity of $\text{Li}_{0.01}\text{M}_{0.05}\text{Ni}_{0.94}\text{O}$ ($M = \text{V}$ and W) ceramics

Guo-Ju Chen^a, Yu-Jen Hsiao^{b,*}, Yee-Shin Chang^c, Yin-Lai Chai^d

^a Department of Materials Science and Engineering, I-Shou University, Kaohsiung 840, Taiwan

^b National Nano Device Laboratories, Tainan 741, Taiwan

^c Institute of Electro-Optical and Materials Science, National Formosa University, Yunlin 632, Taiwan

^d Department of Environmental Resources Management, Dahan Institute of Technology, Hualien 971, Taiwan

ARTICLE INFO

Article history:

Received 27 December 2007

Received in revised form 11 June 2008

Accepted 15 June 2008

Available online 3 August 2008

Keywords:

Polarization

Dielectric

NiO

Solid-state reaction

ABSTRACT

Microstructure and dielectric behavior of $\text{Li}_{0.01}\text{M}_{0.05}\text{Ni}_{0.94}\text{O}$ ($M = \text{V}$ and W) ceramics were studied. The contents of V_2O_5 and WO_3 were mainly dispersed into the grain boundaries and existed as the $\text{Ni}_3\text{V}_2\text{O}_8$ and NiWO_4 phase. The compounds exhibit a negative temperature coefficient of resistance (NTCR) behavior. The dc conductivity of activation energy for the compositions with $M = \text{V}$ and W are 0.274 and 0.229 eV. The dielectric constant was decreased toward higher frequencies at room temperature. It is the barrier layer capacitors (BLCs) mechanism and the existing large polarization that can cause the high dielectric constant in $\text{Li}_{0.01}\text{M}_{0.05}\text{Ni}_{0.94}\text{O}$ ($M = \text{V}$ and W) ceramics.

© 2008 Elsevier B.V. All rights reserved.

1. Introduction

High dielectric constant materials were found in doping ferroelectric perovskite oxides near the Curie temperature (T_c) such as lead zirconia–titanate (PZT), and ferroelectric-based oxides (PLZT) [1–3]. Recently, another perovskite-related material $\text{CaCu}_3\text{Ti}_4\text{O}_{12}$ (CCTO) [4] and nonperovskite materials Li and Ti codoped NiO based [5,6] and $\text{Li}_{0.01}\text{Ta}_{0.05}\text{Ni}_{0.94}\text{O}$ (LTNO) [7] ceramics have been reported for its unusual high dielectric constant of 10^4 – 10^5 at room temperature, and ascribed to the origin of the high permittivity to extrinsic mechanisms such as the formation of boundary-layer capacitors. High-capacitance ceramic capacitors with barrier layer capacitors (BLCs) and multilayer ceramic capacitors (MLCC) structures have great potential for attaining high-density charge storage. Raevski et al. [8] reported high dielectric permittivity in nonferroelectric perovskite $\text{AFe}_{1/2}\text{B}_{1/2}\text{O}_3$ ceramics ($A = \text{Ba}, \text{Sr}, \text{Ca}$; $B = \text{Nb}, \text{Ta}, \text{Sb}$) in a wide temperature interval, and proposed that the phenomenon of the high dielectric permittivity is due to the Maxwell–Wagner relaxation. Generally, the Maxwell–Wagner polarization, also known as interfacial polarization, has been most widely adopted to explain the high permittivity observed in the materials, including single-phase ceramics or multiphase composites, which often arises in a

material consisting of grains which become semiconducting while grain boundaries are insulating [9,10].

In this report, a nonferroelectric and nonperovskite high permittivity materials, $\text{Li}_{0.01}\text{M}_{0.05}\text{Ni}_{0.94}\text{O}$ ($M = \text{V}$ and W) ceramics have been successfully synthesized. The high dielectric behavior observed in composites is similar to that observed recently in perovskite-like CCTO. It has been suggested that the high dielectric constant response of $\text{Li}_{0.01}\text{M}_{0.05}\text{Ni}_{0.94}\text{O}$ ($M = \text{V}$ and W) could be arisen from the interfacial space charge polarization mechanism.

2. Experimental procedures

The compounds used in this investigation were prepared using a conventional solid-state reaction technique, and the starting materials Li_2CO_3 , NiO, V_2O_5 , and WO_3 have a purity of at least 99.9%. Specimens with the nominal composition of $\text{Li}_{0.01}\text{M}_{0.05}\text{Ni}_{0.94}\text{O}$ ($M = \text{V}$ and W) were prepared. The powders were mixed and ground with acetone in a zirconium oxide ball mill for 24 h. The mixed powders of $\text{Li}_{0.01}\text{V}_{0.05}\text{Ni}_{0.94}\text{O}$ and $\text{Li}_{0.01}\text{W}_{0.05}\text{Ni}_{0.94}\text{O}$ were calcined at 1173 and 1373 K for 2 h in air, respectively. The calcined powders were ground and pressed at 200 MPa into discs with diameters of 10–11 mm and thicknesses of 2–3 mm. The discs of $\text{Li}_{0.01}\text{V}_{0.05}\text{Ni}_{0.94}\text{O}$ and $\text{Li}_{0.01}\text{W}_{0.05}\text{Ni}_{0.94}\text{O}$ were sintered in air at 1373 and 1573 K for 4 h, respectively. Sintered discs were cleaned by N_2 gas and gold was deposited on the surfaces for microstructural observation. The electrodes for dielectric measurements were deposited on the ground disk surface by rubbing on an In–Ga alloy.

Structure and the lattice parameters of the samples were determined by X-ray powder diffraction (Rigaku D/max) with $\text{Cu K}\alpha$ radiation at room temperature. The grain morphology and grain size were characterized by scanning electron microscopy (SEM, Hitachi S-3000N, Japan). The dielectric constants and dielectric loss were measured from 50 Hz to 1 MHz using an LCR meter (HP4284A) at room

* Corresponding author. Tel.: +886 6 2757575x62968; fax: +886 6 2382800.
E-mail address: ken@mail.mse.ncku.edu.tw (Y.-J. Hsiao).

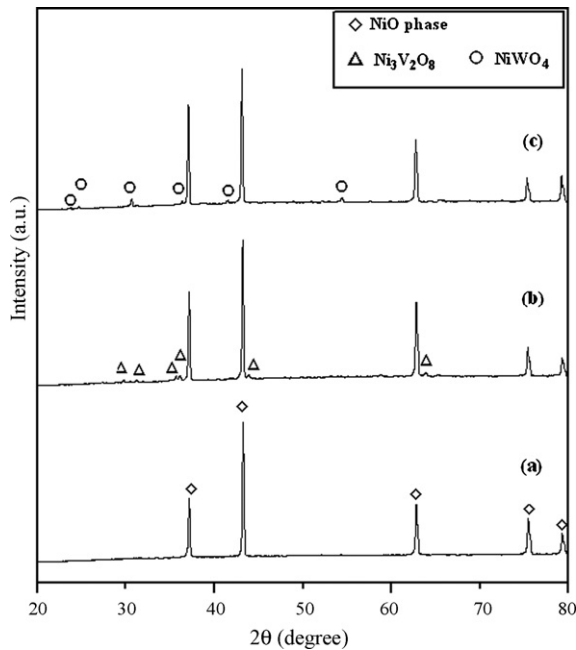


Fig. 1. X-ray diffraction patterns for compositions (a) $\text{Li}_{0.01}\text{Ni}_{0.99}\text{O}$, (b) $\text{Li}_{0.01}\text{Ni}_{0.94}\text{V}_{0.05}\text{O}$, and (c) $\text{Li}_{0.01}\text{Ni}_{0.94}\text{W}_{0.05}\text{O}$ ceramics.

temperature. The resistivity (ρ , $\Omega\text{-cm}$) values of the sintered samples were measured from the impedance analyzer (HP3457A).

3. Results and discussion

3.1. Crystal structure

The X-ray diffraction patterns of the various composition of $\text{Li}_{0.01}\text{M}_{0.05}\text{Ni}_{0.94}\text{O}$ ($M=\text{V}$ and W) are shown in Fig. 1. The $\text{Li}_{0.01}\text{Ni}_{0.99}\text{O}$ ceramic was pure cubic phase. When 5% V_2O_5 , and WO_3 were substituted for the $\text{Li}_{0.01}\text{Ni}_{0.99}\text{O}$ ceramic, it showed small amount of second phases of $\text{Ni}_3\text{V}_2\text{O}_8$ and NiWO_4 , respectively. The samples exhibited two phases in the composites ($M=\text{V}$ and W), i.e. their diffraction peaks from the cubic phase of NiO and second phases of $\text{Ni}_3\text{V}_2\text{O}_8$ and NiWO_4 , which corresponds to the cards of JCPDS were observed. No peak shift was observed indicating a lack of mutual solubility between the two phases. The lattice constants were determined from the diffraction patterns using a computer program called *Unit Cell*. They are almost constant of the lattice parameter $a=4.19\text{ \AA}$ of the NiO cubic phase in the compositions with $M=\text{V}$ and W .

Scanning electron microscopy (SEM) pictures of the samples $\text{Li}_{0.01}\text{M}_{0.05}\text{Ni}_{0.94}\text{O}$ ($M=\text{V}$ and W) are shown in Fig. 2a and b, respectively. Dense, two-phase microstructures of the sintered composites are evident. It can be seen clearly that the grains of second phase were significantly showed for doping various oxides (V_2O_5 and WO_3). The NiO phase appears as the matrix grain with obvious grain boundary and accompanies small secondary phase on grain surface or boundary. Second phase of rod-like grains with diameter $0.5\text{--}1\text{ }\mu\text{m}$ appeared on the $\text{Li}_{0.01}\text{V}_{0.05}\text{Ni}_{0.94}\text{O}$ pellet in Fig. 2a, that corresponded to the formation of $\text{Ni}_3\text{V}_2\text{O}_8$ phase from XRD. A similar phenomenon was also observed in the $\text{Li}_{0.01}\text{W}_{0.05}\text{Ni}_{0.94}\text{O}$ ceramic in Fig. 2b. The second phase of NiWO_4 rod-grains are lay down on the surface of large NiO grains, NiO and NiWO_4 forming an interface with ripple-like morphology. In the sintering process, for low doping levels, an atom attempting a jump will, therefore, be come unstable and be forced back to its original position. It can thus be seen that continuous growth at the

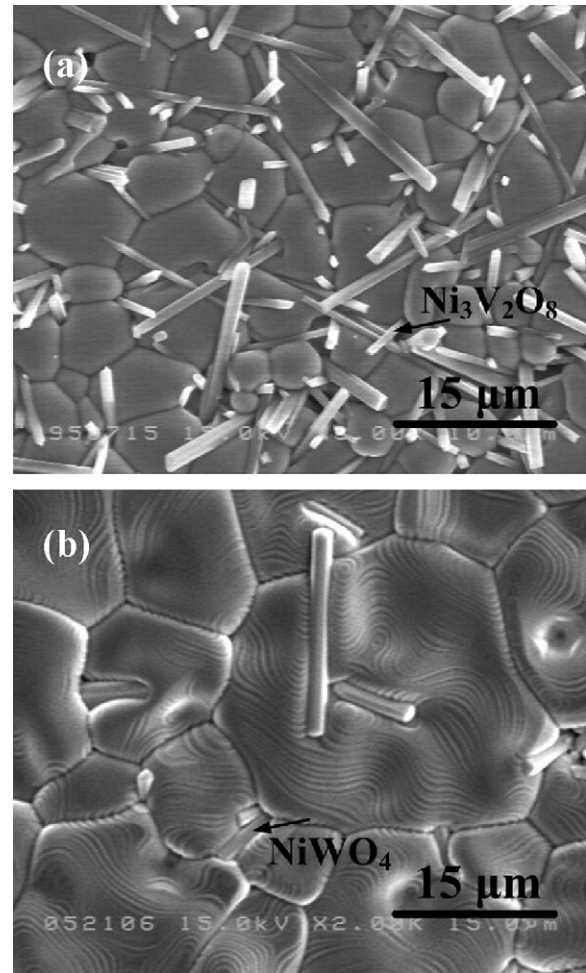


Fig. 2. The SEM pictures of the surfaces with (a) $\text{Li}_{0.01}\text{Ni}_{0.94}\text{V}_{0.05}\text{O}$ and (b) $\text{Li}_{0.01}\text{Ni}_{0.94}\text{W}_{0.05}\text{O}$ ceramics.

above type of interfaces will be very difficult. A way of avoiding the difficulties of continuous growth encountered in the above case is provided by the 'ledge' mechanism [11]. This reason may be cause ripple effect on the large NiO grains.

3.2. Electrical conductivity

The values of the electrical resistivity at room temperature for the compositions with $M=\text{V}$ and W were of the order of 5.2×10^6 and 3.8×10^5 ($\Omega\text{-cm}$), respectively. The nature of the curve shows that the resistivity decreases with increasing temperature, which suggests that the negative temperature coefficient of the resistivity (NTCR) exists in these compounds. The variation of total dc conductivity (σ_{dc}) total against inverse of absolute temperature (10^3 K^{-1}) at a constant biasing field is shown in Fig. 3. The nature of variation is almost linear indicating ohmic type and obeys the Arrhenius relation [12],

$$\sigma = \sigma_0 \exp\left(\frac{-E_a}{K_B T}\right) \quad (1)$$

where σ_0 represents a pre-exponential factor, K_B is the Boltzmann constant, E_a is the activation energy and T is the absolute temperature. This nature of the curve shows that conductivity increases with temperature, which means the resistivity decreases. The decrease in resistivity at high temperature may be due to the supply of more and more energy to the material as the tempera-

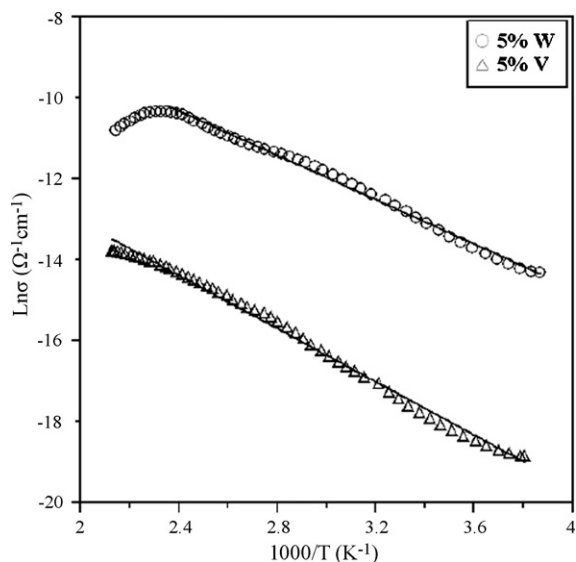


Fig. 3. Activation energy was evaluated according to the straight-line segments of conductivity (σ) vs. reciprocal temperature.

ture increases. The value of E_a has been estimated from the slope of $\ln \sigma$ versus T^{-1} , plot in approximation of a straight line. The value of E_a of the compositions with $M=V$ and W are 0.274 and 0.229 eV, respectively.

3.3. Dielectric properties

As shown in Fig. 4a, an almost linear curve for $W=5\%$ and step-like curve for $V=5\%$ were observed in the samples. These curves decrease the dielectric constant toward higher frequencies at room temperature. The sample of $V=5\%$ has the lower dielectric constant than the $\text{Li}_{0.01}\text{W}_{0.05}\text{Ni}_{0.94}\text{O}$ sample. It is noteworthy that the dielectric constant is about three to four orders of magnitude higher than that in pure NiO ceramics (~ 30) at 1 kHz [13]. The inset of Fig. 4a shows the variation of dielectric loss ($\tan \delta$) as a function of frequency at room temperature. In Fig. 4b, dielectric constant and dielectric loss at 10 kHz for W and $V=5\%$ vs temperature (T) are also shown. It should be noted that ϵ_r increase with the temperature increasing. In addition, the feature of the peak is observed in $\tan \delta$ vs temperature plots at 295 and 410 K for W and V doped NiO-based ceramics. The sample of $V=5\%$ has the higher dielectric loss than the $\text{Li}_{0.01}\text{W}_{0.05}\text{Ni}_{0.94}\text{O}$ sample. The losses of $W=5\%$ are always lower than 1 with the frequencies. The dielectric loss is also lower than other high permittivity oxides, such as $\text{CaCu}_3\text{Ti}_4\text{O}_{12}$ -based [14] and $\text{BaFe}_{0.5}\text{Nb}_{0.5}\text{O}_3$ -based ceramics [15].

Such a obviously increase in the value of the dielectric constant at lower frequencies and higher temperatures can be explained in terms of the interfacial space charge polarization. In addition, Li et al. [16] observed the dielectric constant in ferromagnetic–ferroelectric mixed composites. They cited the Maxwell–Wagner polarization, also called interfacial polarization, from the formation of heterogeneous structures. In addition, it has been known that addition of dopants to ferroelectric perovskites can lead to greatly enhanced dielectric constants through the barrier layer capacitors (BLCs) mechanism [17]. Thus, defects could be very different in these samples, which could have a great influence on the dielectric constant (ϵ_r) due to the boundary layer.

NiO is a Mott–Hubbard insulator at room temperature, but doping with monovalent cations like Li^+ can cause considerable increase in the conductivity of NiO, and thus NiO becomes semi-conducting due to these defects [18]. For the $W=5\%$ sample, $\text{V}_\text{O}^\bullet$

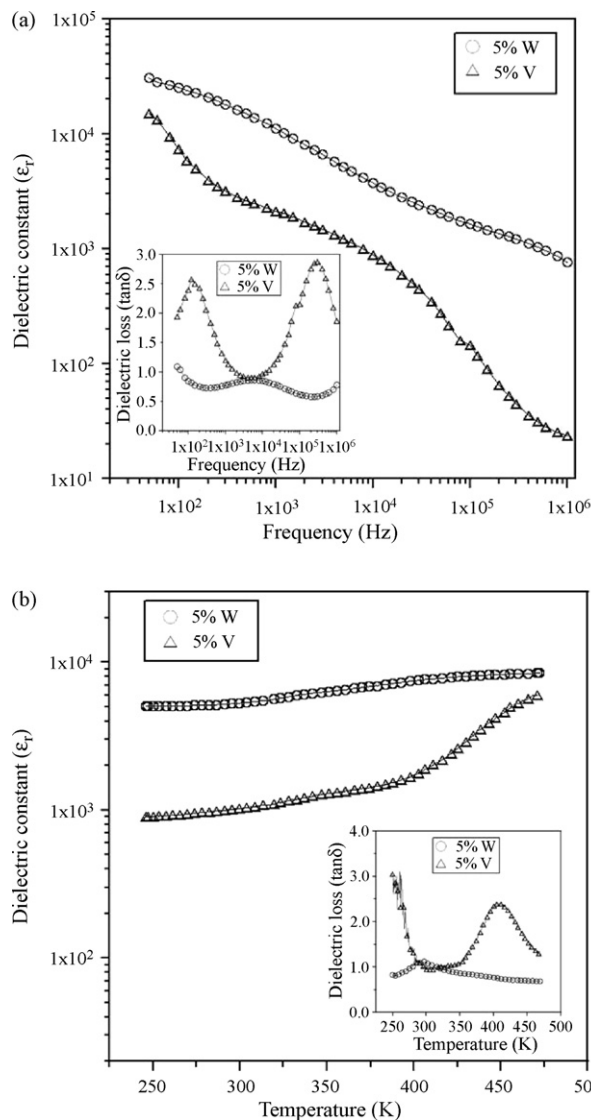


Fig. 4. (a) Frequency and (b) temperature dependence of the dielectric constant (ϵ_r) and the inset is the dielectric loss ($\tan \delta$) for $\text{Li}_{0.01}\text{Ni}_{0.94}\text{M}_{0.05}\text{O}$ ($M=V$, and W) ceramics.

combine with $2\text{Li}_{\text{Ni}^{2+}}^{1+}$ will form dipoles due to the coulombic attraction. These defect dipoles can probably be represented as $2\text{Li}_{\text{Ni}^{2+}}^{1+} - \text{V}_\text{O}^\bullet$. Normally, the dielectric permittivity is proportional to the intensity of the polarization. Therefore, the higher polarization is in agreement with the dependence of the dielectric constant on the sample of the concentrations $W=5\%$.

The impedance measurements were performed at room temperature and are shown in Fig. 5a and b. It depicts the Cole–Cole impedance plots for $W=5\%$ in Fig. 5a, and two depressed circular arcs are combined to form a big circular arc, corresponding to the contributions of two separate dielectric polarization processes. The big circular arc at the lower frequency corresponds to the grain boundaries, which is mainly space charge polarization, while the one at the higher frequencies corresponds to the orientational polarization of the grain. Measuring the sample of $V=5\%$ (Fig. 5b), third depressed circular arc is further found, this contributed to the electrode-specimen interface polarization effect at lower frequencies [19]. It is the barrier layer capacitors (BLCs) mechanism and the existing large polarization that cause the high dielectric constant in $\text{Li}_{0.01}\text{M}_{0.05}\text{Ni}_{0.94}\text{O}$ ($M=V$ and W) ceramics. In this inves-

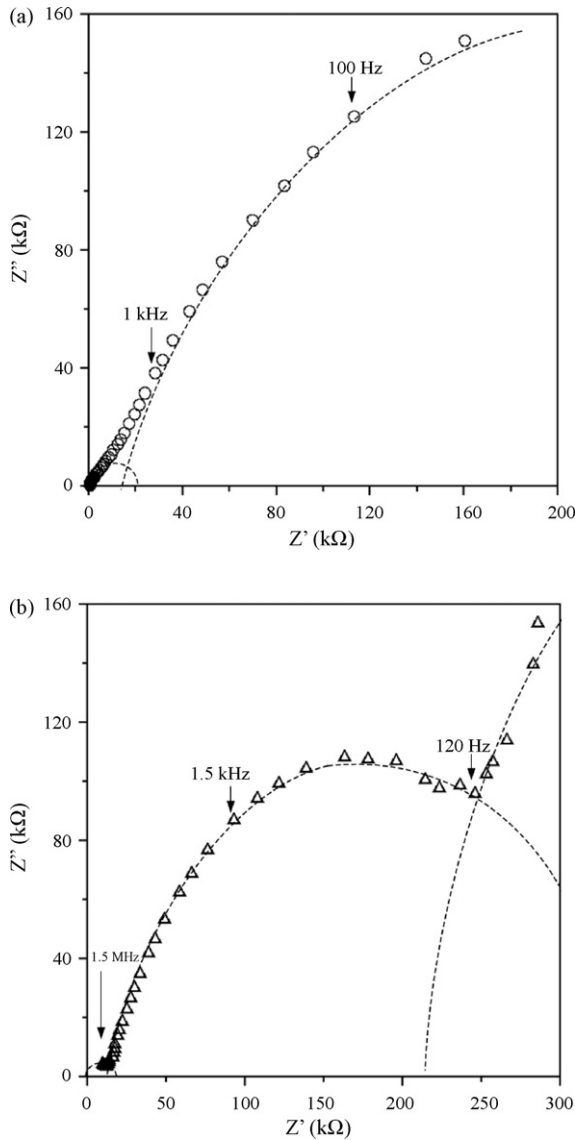


Fig. 5. Cole–Cole impedance plots for the samples (a) $\text{Li}_{0.01}\text{Ni}_{0.94}\text{W}_{0.05}\text{O}$ and (b) $\text{Li}_{0.01}\text{Ni}_{0.94}\text{V}_{0.05}\text{O}$, ceramics were measured at room temperature.

tigation, one important thing was observed, *i.e.* the higher value of the dielectric constant was due to the formation of barriers with the space charge and interface polarization, and that was affected by the lower frequencies at a fixed temperature.

4. Conclusions

Two nominal compositions of $\text{Li}_{0.01}\text{M}_{0.05}\text{Ni}_{0.94}\text{O}$ ($M = \text{V}$ and W) ceramics were prepared. The dopants of V_2O_5 and WO_3 were mainly dispersed into the grain boundaries and existed as the $\text{Ni}_3\text{V}_2\text{O}_8$ and NiWO_4 phase by XRD and SEM results, which had a great influence on the dielectric properties. The dc conductivity of the activation energy (E_a) of the compositions with $M = \text{V}$ and W are 0.274 and 0.229 eV, respectively. It is the barrier layer capacitors (BLCs) mechanism and the existing large polarization that cause the high dielectric constant in $\text{Li}_{0.01}\text{M}_{0.05}\text{Ni}_{0.94}\text{O}$ ($M = \text{V}$ and W) ceramics.

Acknowledgment

The authors express their thanks to the National Science Council of Taiwan for supporting this work with a grant under the contract of 96-2811-E-006-014.

References

- [1] S.R. Shannigrahi, R.N.P. Choudhary, H.N. Acharya, Mater. Res. Bull. 34 (1999) 1875.
- [2] S. Dutta, R.N.P. Choudhary, P.K. Sinha, J. Alloys Comp. 426 (2006) 345.
- [3] S. Dutta, R.N.P. Choudhary, P.K. Sinha, J. Alloys Comp. 430 (2007) 344.
- [4] T.B. Adams, D.C. Sinclair, A.R. West, Adv. Mater. 14 (2002) 1321.
- [5] J. Wu, C.-W. Nan, Y.H. Lin, Y. Deng, Phys. Rev. Lett. 89 (2002) 217601.
- [6] Y.H. Lin, M. Li, C.-W. Nan, J. Li, J. Wu, J. He, Appl. Phys. Lett. 89 (2006) 032907.
- [7] Y.J. Hsiao, Y.S. Chang, T.H. Fang, Y.L. Chai, C.Y. Chung, Y.H. Chang, J. Phys. D: Appl. Phys. 40 (2007) 863.
- [8] I.P. Raevski, S.A. Prosandeev, A.S. Bogatin, M.A. Malitskaya, L. Jastrabik, J. Appl. Phys. 93 (2003) 4130.
- [9] Y.J. Hsiao, Y.H. Chang, T.H. Fang, Y.S. Chang, Y.L. Chai, J. Alloys Comp. 421 (2006) 240.
- [10] Y.H. Lin, L. Jiang, R.J. Zhao, C.-W. Nan, Phys. Rev. B 72 (2005) 014103.
- [11] C.Y. Chung, Y.H. Chang, Y.S. Chang, G.J. Chen, J. Alloys Comp. 385 (2004) 298.
- [12] Y.J. Hsiao, Y.H. Chang, T.H. Fang, Y.S. Chang, Y.L. Chai, Mater. Lett. 60 (2006) 3655.
- [13] Y.H. Lin, R.J. Zhao, J.F. Wang, J. Cai, C.-W. Nan, J. Am. Ceram. Soc. 88 (2005) 1808.
- [14] S. Guillemet-Fritsch, T. Lebey, M. Boulos, B. Durand, J. Eur. Ceram. Soc. 26 (2006) 1245.
- [15] C.Y. Chung, Y.H. Chang, G.J. Chen, J. Appl. Phys. 96 (2004) 6624.
- [16] Y.J. Li, X.M. Chen, R.Z. Hou, Y.H. Tang, Solid-State Commun. 137 (2006) 120.
- [17] C.F. Yang, Jpn. J. Appl. Phys. 35 (1996) 1806.
- [18] J. Van Elp, H. Eskes, P. Kuiper, G.A. Sawatzky, Phys. Rev. B 45 (1992) 1612.
- [19] Y.J. Hsiao, Y.H. Chang, T.H. Fang, Y.S. Chang, Y.L. Chai, J. Appl. Phys. 99 (2006) 064104.